A relevant question for discussion is whether Au–Au bonding interactions contribute to the unique structure of Au₄(dta)₄. The Au–Au mean distance of 3.013 Å in this compound, when compared with those in the metal, 2.884 Å,[15] and in the periphery of unbridged cluster compounds such as [Au₆(PPh₃)₆]²⁺, 3.02 Å,[45] and Au₁₁I₃[P(p-C₆H₄F)₃]₇, 2.98 Å[46] (recent MO calculations[47] indicate an important peripheral bonding in these clusters), would seem to suggest attractive Au–Au interactions, possibly as a result of the ability of the dithioacetato ligand system to encourage d–s orbital mixing on gold and to dissipate antibonding density from the plane of the cluster through its delocalized π virtual orbitals.[21]

The Mössbauer results for the tetramer, however, do not provide evidence in support of this view. It has been found[48-53] that an almost linear correlation exists between the isomer shift and quadrupole splitting parameters pertaining to mononuclear, linearly coordinated gold(I) compounds. Figure 4 shows that the values obtained for Au₄(dta)₄ appear to follow the same isomer shift/quadrupole splitting relation. Therefore, the Mössbauer results do not give any indication of the presence of direct interactions between the gold atoms of the tetramer. On the other hand, Figure 4 shows that the same conclusion holds for, e.g., the gold atoms in [Au(i-C₄H₉)₂NCS₂]₂ (with an Au–Au distance of 2.76 Å, shorter than that in metallic gold, and for which a bond

order of ca. 0.25 has been estimated by Raman spectroscopy[13,54]) or the gold atoms in the periphery of gold clusters like Au₈-(PPh₃)₈²⁺ (with peripheral Au–Au distances in the range 2.826 (8)–2.960 (8) Å.[55] The fact that gold atoms can come rather close without showing any interaction in the Mössbauer spectrum might introduce some doubt on the capability of the technique in detecting minor bonding effects. It may be significant, in this respect, that the photoelectron spectra of AuMe(PMe₃) have revealed (in agreement with Xα calculations) a significant Au 5d character in the Au–P bond,[56] a feature that is not evident from the Mössbauer parameters pertaining to a variety of phosphine complexes of gold(I).[49] The involvement of the Au 5d orbitals in bonding is, of course, a prerequisite to any attractive Au(I)–Au(I) interaction.

(45) Bellon, P.; Manassero, M.; Sansoni, M. *J. Chem. Soc., Dalton Trans.* **1973**, 2423.
(46) Bellon, P.; Manassero, M.; Sansoni, M. *J. Chem. Soc., Dalton Trans.* **1972**, 1481.
(47) Mingos, D. M. P. *J. Chem. Soc., Dalton Trans.* **1976**, 1163.
(48) Faltens, M. P.; Shirley, D. A. *J. Chem. Phys.* **1970**, *53*, 4249.
(49) Jones, P. G.; Maddock, A. G.; Mays, M. J.; Muir, M. M.; Williams, A. F. *J. Chem. Soc., Dalton Trans.* **1977**, 1434.
(50) Charlton, J. S.; Nichols, D. I. *J. Chem. Soc. A* **1970**, 1484.
(51) McAuliffe, C. A.; Parish, R. V.; Randall, P. D. *J. Chem. Soc., Dalton Trans.* **1977**, 1426.
(52) Viegers, M. P. A. Ph.D. Thesis, Catholic University of Nijmegen, Nijmegen, The Netherlands, 1976.
(53) Hill, D. T.; Sadler, P. J.; Calis, G.; Trooster, J. M. In "Bioinorganic Chemistry of Gold Coordination Compounds"; Sutton, B. M., Ed.; Smith Kline & French Laboratories: Philadelphia, 1983; p 67.

(54) A reviewer informed us that a frequency of 105 cm⁻¹ in the Raman spectrum of [Au(i-C₄H₉)₂NCS₂]₂ is a more reliable assignment for the Au–Au stretching mode than the value of 185 cm⁻¹ reported by Farrell and Spiro in ref 13 and that, therefore, the assignment for the bond order of 0.25 should be modified.
(55) Vollenbroek, F. A.; Bosman, W. P.; Bour, J. J.; Noordik, J. H.; Beurskens, P. T. *J. Chem. Soc., Chem. Commun.* **1979**, 387.
(56) Bancroft, G. M.; Chan, T.; Puddephatt, R. J.; Tse, J. S. *Inorg. Chem.* **1982**, *21*, 2946.
(57) Viegers, M. P. A.; Trooster, J. M.; Bouten, P.; Rit, T. P. *J. Chem. Soc., Dalton Trans.* **1977**, 2074.
(58) Vollenbroek, F. A. Ph.D. Thesis, Catholic University of Nijmegen, The Netherlands, 1979.

Contribution from the Department of Chemistry, The University of Michigan, Ann Arbor, Michigan 48109, and the Molecular Structure Center, Indiana University, Bloomington, Indiana 47405

Synthesis and Properties of Ditungsten(II) Tetracarboxylates[1]

D. J. SANTURE,[2a] J. C. HUFFMAN,[2b] and A. P. SATTELBERGER*[2a,c]

Synthetic procedures affording yellow W₂(O₂C-t-Bu)₄ and W₂(O₂CMe)₄ in good yields are described. The pivalate dimer was prepared by reduction of [WCl₄]ₓ in THF with sodium amalgam in the presence of NaO₂C-t-Bu. An analogous reaction with sodium acetate failed to provide W₂(O₂CMe)₄. The latter was prepared by metathesis of W₂(O₂CCF₃)₄ with tetrabutylammonium acetate in toluene. Both of the alkanecarboxylate dimers are extremely air sensitive, especially in solution. They have been characterized by IR, Raman, and mass spectroscopy. An axial triphenylphosphine adduct of the pivalate dimer, W₂(O₂C-t-Bu)₄·2PPh₃, has been characterized by low-temperature (−160 °C) X-ray crystallography: monoclinic space group C2/c, a = 27.537 (12) Å, b = 9.543 (4) Å, c = 29.131 (14) Å, β = 133.93 (1)°, Z = 4. The structure refined to residuals of R_F = 5.89% and R_{wF} = 4.42%. The molecule resides on an inversion center, and the W–W distance is 2.218 (1) Å. The electrochemical properties of W₂(O₂C-t-Bu)₄ and W₂(O₂CMe)₄ have been investigated by cyclic voltammetry in CH₃CN solution and are compared to those of Mo₂(O₂C-t-Bu)₄ and Mo₂(O₂C-n-Pr)₄. Paramagnetic, gray [W₂(O₂C-t-Bu)₄]I has been obtained from the reaction of the pivalate dimer with I₂ in benzene solution and characterized by IR and ESR spectroscopy. The visible absorption spectra of W₂(O₂CCF₃)₄ and W₂(O₂C-t-Bu)₄ (THF solution) have been studied and are compared to the spectra of the molybdenum analogues and MoW(O₂C-t-Bu)₄.

Introduction

The molybdenum(II) carboxylates, Mo₂(O₂CR)₄, are the most important compounds containing molybdenum–molybdenum quadruple bonds. First reported in the early 1960s by Wilkinson

and co-workers,[3] they remain the key starting materials in Mo₂⁴⁺ chemistry and have been the objects of numerous physical and theoretical studies.[4] The most commonly used method of preparation is the thermal reaction of Mo(CO)₆ with a carboxylic acid, either neat or, preferably, in an inert solvent such as diglyme or

(1) Metal–Metal Bonded Complexes of the Early Transition Metals. 9. Part 8: Santure, D. J.; Huffman, J. C.; Sattelberger, A. P. *Inorg. Chem.* **1984**, *23*, 938.
(2) (a) The University of Michigan. (b) Indiana University. (c) Present address: Los Alamos National Laboratory, Los Alamos, NM 87545.

(3) Stephenson, T. A.; Bannister, E.; Wilkinson, G. *J. Chem. Soc.* **1964**, 2538.
(4) Cotton, F. A.; Walton, R. A. "Multiple Bonds Between Metal Atoms"; Wiley: New York, 1982.

o-dichlorobenzene. Excellent yields of $Mo_2(O_2CR)_4$ can be obtained by this procedure. A logical extension of the molybdenum(II) carboxylate synthesis is the substitution of $W(CO)_6$ for $Mo(CO)_6$ to prepare $W_2(O_2CR)_4$ compounds. Such reactions have been performed many times, under varied conditions, in numerous laboratories.[4] They provide trinuclear tungsten(IV) species, e.g., $[W_3O_2(O_2CMe)_6(H_2O)_3]^{2+}$, without any indication that W_2-$(O_2CR)_4$ compounds are ever formed.[5]

The first authentic tungsten(II) dimers were reported in 1977. Using methyllithium as a ligand source and reductant in reactions with WCl_4 or WCl_5, Cotton et al.[6] isolated lithium salts of $W_2Me_8^{4-}$ and $W_2Cl_nMe_{8-n}^{4-}$. In that paper, the authors noted that the reaction between $W_2Me_8^{4-}$ and HO_2CMe (≥ 4 equiv) failed to provide $W_2(O_2CMe)_4$. In 1980, Sharp and Schrock[7] prepared a series of $W_2Cl_4(PR_3)_4$ complexes. Their attempt to prepare $W_2(O_2CMe)_4$ from the reaction of $W_2Cl_4(PBu_3)_4$ and acetic acid was also unsuccessful. In 1981, 16 years after the crystal structure of $Mo_2(O_2CMe)_4$ was published,[8] the ditungsten tetracarboxylate mystery was finally solved.[9] Abandoning procedures that involved potential oxidizing agents, we discovered that the reduction of WCl_4 in tetrahydrofuran in the presence of a sodium carboxylate provided these long-sought tungsten(II) dimers. In our initial paper[9] and several subsequent contributions,[1,10,11] we focused our attention on the trifluoroacetate derivative, $W_2(O_2CCF_3)_4$, an air-sensitive, thermally stable, yellow crystalline compound, which is easily obtained in yields exceeding 50%. A crystal structure of $W_2(O_2CCF_3)_4\cdot^2/_3(\text{diglyme})$ confirmed the presence of an authentic $M_2(O_2CR)_4$ core.[9]
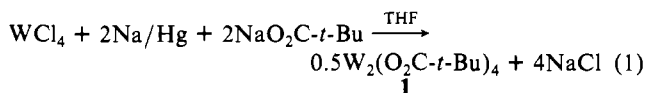
Soon after the preparation of $W_2(O_2CCF_3)_4$, we isolated tungsten(II) pivalate, $W_2(O_2C\text{-}t\text{-Bu})_4$, using a variant of the original procedure.[9] Cotton and Wang, working independently and using the "reducing salt method", isolated the benzoate derivative, $W_2(O_2CPh)_4$, several months later,[12] and it appeared that the synthesis was a general one. These optimistic thoughts were soon dashed by our inability to prepare tungsten(II) acetate or tungsten(II) formate. After a considerable amount of time and effort, the former dimer was successfully isolated by a new procedure, which is described below.

The availability of three different alkanecarboxylate dimers made several physical studies possible and desirable. In addition to the crystal structure of $W_2(O_2C\text{-}t\text{-Bu})_4\cdot2PPh_3$, we report here (1) cyclic voltammetry experiments that provide a rationale for the oxidative instability of $W_2(O_2CR)_4$ compounds, (2) the isolation and ESR spectrum of $[W_2(O_2C\text{-}t\text{-Bu})_4]I$, a $\sigma^2\pi^4\delta^1$ species, and (3) the electronic absorption spectra of the alkanecarboxylate dimers.

Results

Preparation of $W_2(O_2CR)_4$ (R = t-Bu, Me) Compounds. Reduction of polymeric tungsten tetrachloride with 2 equiv of sodium amalgam in the presence of 2 equiv of sodium pivalate ($NaO_2C\text{-}t\text{-Bu}$) provides deep yellow-brown solutions containing $W_2(O_2C\text{-}t\text{-Bu})_4$ (1) (reaction 1). The latter can be isolated as

$$WCl_4 + 2Na/Hg + 2NaO_2C\text{-}t\text{-Bu} \xrightarrow{\text{THF}}$$
$$0.5W_2(O_2C\text{-}t\text{-Bu})_4 + 4NaCl \quad (1)$$
$$\mathbf{1}$$

a yellow powder after solvent removal, extraction of the solid

Table I. Crystal Data for $W_2(O_2C\text{-}t\text{-Bu})_4\cdot2PPh_3$

mol formula	$W_2O_8P_2C_{56}H_{66}$
color	yellow-orange
cryst dimens, mm	$0.07 \times 0.08 \times 0.07$
space group	$C2/c$
cell dimens[a]	
a, Å	27.537 (12)
b, Å	9.543 (4)
c, Å	29.131 (14)
β, deg	133.93 (1)
molecules/cell	4
cell V, Å^3	5513.2
d(calcd), g cm^{-3}	1.562
λ, Å	0.710 69
mol wt	1296.79
linear abs coeff, cm^{-1}	43.65
2θ range, deg	6–45
no. of data with $F_0 > 2.33\sigma(F_0)$	2769
no. of unique data	3635
final residuals: R_F, R_{wF}	0.0589, 0.0442
goodness of fit, last cycle	1.253
max Δ/σ, last cycle	0.05

[a] At -163 °C; 32 reflections.

residue with hot toluene, filtration of the resulting mixture, reduction of the filtrate volume, and cooling to -40 °C. Beautiful bright yellow needles are obtained on recrystallization of the crude product from fresh toluene. The yields of purified dimer are typically in the 60–65% range, based on WCl_4.

The procedure just described is similar to, but not identical with, those used to prepare $W_2(O_2CCF_3)_4$[11] and $W_2(O_2CPh)_4$.[12] On the basis of these results, it might be anticipated that tungsten(II) acetate, $W_2(O_2CMe)_4$ (2), would form if sodium acetate was used as a carboxylate source. In fact, this is not the case; reduction of WCl_4 in the presence of NaO_2CMe failed to provide any 2. Subsequent experiments with a THF-soluble acetate source, viz., tetrabutylammonium acetate, were likewise unsuccessful. Eventually, a simple and straightforward route to 2, based on carboxylate ligand exchange, was developed. The addition of tetrabutylammonium acetate (4–5 equiv) to a warm concentrated toluene solution of freshly sublimed $W_2(O_2CCF_3)_4$ results in the immediate precipitation of a yellow powder (reaction 2). The

$$W_2(O_2CCF_3)_4 + 4[Bu_4N]O_2CMe \xrightarrow{\text{PhCH}_3}$$
$$W_2(O_2CMe)_4 + 4[Bu_4N]O_2CCF_3 \quad (2)$$
$$\mathbf{2}$$
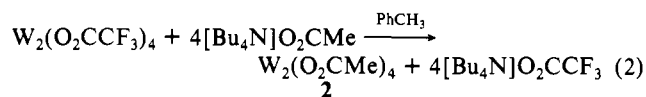
latter is filtered off, washed successively with methylene chloride and hexane, and dried in vacuo. This procedure provides pure 2 in ca. 80% yield, based on the trifluoroacetate dimer.

The successful isolation of 1 and 2 prompted a search for X-ray-quality crystals of either material. Regrettably, neither sublimation in a sealed, evacuated tube (cf. $Mo_2(O_2C\text{-}t\text{-Bu})_4$[13]) nor recrystallization from a variety of solvents, including o-dichlorobenzene,[14] provided us with suitable samples. We then turned our attention to the synthesis of axially substituted derivatives, and our efforts were rewarded in the form of W_2-$(O_2C\text{-}t\text{-Bu})_4\cdot2PPh_3$ (3). The latter was prepared in high yield by adding triphenylphosphine to concentrated toluene solutions of the parent (reaction 3). Compound 3 formed clear yellow-orange

$$W_2(O_2C\text{-}t\text{-Bu})_4 + 2PPh_3 \xrightarrow{\text{PhCH}_3} W_2(O_2C\text{-}t\text{-Bu})_4\cdot2PPh_3 \quad (3)$$
$$\mathbf{1} \qquad\qquad\qquad\qquad\qquad \mathbf{3}$$

crystals, suitable for diffraction studies (vide infra), on recrystallization from hot toluene. X-ray-quality adducts (e.g., THF, PPh$_3$) of 2 have eluded us thus far.

Solid-State Structure of $W_2(O_2C\text{-}t\text{-Bu})_4\cdot2PPh_3$. Crystal data for 3 are given in Table I. Positional and isotropic thermal parameters are presented in Table II. Selected interatomic

(5) Bino, A.; Cotton, F. A.; Dori, Z.; Koch, S.; Küppers, H.; Millar, M.; Sekutowski, J. C. *Inorg. Chem.* **1978**, *17*, 3245.

(6) Cotton, F. A.; Koch, S.; Mertis, K.; Millar, M.; Wilkinson, G. *J. Am. Chem. Soc.* **1977**, *99*, 4989.

(7) Sharp, P. R.; Schrock, R. R. *J. Am. Chem. Soc.* **1980**, *102*, 1430.

(8) Lawton, D.; Mason, R. *J. Am. Chem. Soc.* **1965**, *87*, 921.

(9) Sattelberger, A. P.; McLaughlin, K. W.; Huffman, J. C. *J. Am. Chem. Soc.* **1981**, *103*, 2880.

(10) Bancroft, G. M.; Pellach, E.; Sattelberger, A. P.; McLaughlin, K. W. *J. Chem. Soc., Chem. Commun.* **1982**, 752.

(11) Santure, D. J.; McLaughlin, K. W.; Huffman, J. C.; Sattelberger, A. P. *Inorg. Chem.* **1983**, *22*, 1877.

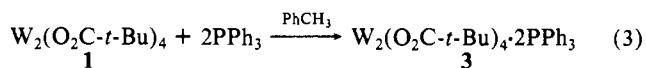(12) Cotton, F. A.; Wang, W. *Inorg. Chem.* **1982**, *21*, 3859.

(13) Cotton, F. A.; Extine, M.; Gage, L. D. *Inorg. Chem.* **1978**, *17*, 172.

(14) Martin, D. S.; Newman, R. A.; Fanwick, P. E. *Inorg. Chem.* **1979**, *18*, 2511.

Table II. Fractional Coordinates and Isotropic Thermal Parameters for $W_2(O_2C$-t-$Bu)_4 \cdot 2PPh_3{}^a$

atom	x	y	z	B_{iso}, Å^2
W(1)	118.9 (2)	−583.5 (5)	4759.0 (2)	16.
P(2)	547 (1)	−1378 (3)	4100 (1)	22
O(3)	384 (3)	−2357 (7)	5307 (3)	21
O(4)	151 (3)	−1186 (7)	5801 (3)	20
O(5)	1124 (3)	90 (8)	5463 (3)	20
O(6)	873 (3)	1269 (7)	5946 (3)	18
C(7)	352 (5)	−2317 (10)	5730 (4)	17
C(8)	515 (6)	−3594 (12)	6110 (5)	30
C(9)	689 (7)	−3169 (13)	6720 (5)	33
C(10)	−113 (8)	−4515 (14)	5695 (6)	45
C(11)	1099 (7)	−4351 (15)	6279 (6)	47
C(12)	1307 (5)	862 (10)	5928 (5)	19
C(13)	2032 (6)	1181 (14)	6464 (5)	30
C(14)	2329 (8)	−159 (18)	6880 (8)	83
C(15)	2395 (9)	1239 (28)	6263 (9)	118
C(16)	2164 (7)	2272 (21)	6888 (8)	79
C(17)	1226 (6)	−2659 (11)	4506 (5)	24
C(18)	1537 (6)	−3084 (12)	4300 (6)	30
C(19)	2069 (6)	−4012 (12)	4652 (6)	32
C(20)	2308 (7)	−4535 (13)	5213 (7)	39
C(21)	2022 (6)	−4115 (13)	5437 (6)	32
C(22)	1474 (5)	−3198 (12)	5083 (5)	25
C(23)	840 (5)	65 (12)	3928 (5)	22
C(24)	1159 (6)	1155 (13)	4354 (6)	30
C(25)	1380 (7)	2339 (15)	4261 (6)	39
C(26)	1268 (7)	2392 (14)	3714 (7)	41
C(27)	947 (7)	1314 (15)	3292 (6)	41
C(28)	735 (6)	142 (14)	3388 (6)	33
C(29)	−174 (6)	−2033 (13)	3295 (5)	27
C(30)	−755 (7)	−1250 (15)	2944 (6)	37
C(31)	−1343 (7)	−1607 (19)	2337 (6)	50
C(32)	−1347 (7)	−2840 (18)	2081 (6)	48
C(33)	−782 (8)	−3657 (16)	2416 (7)	47
C(34)	−174 (6)	−3301 (14)	3047 (5)	33

^{a} Fractional coordinates are $\times 10^4$. B_{iso} values are $\times 10$. Isotropic values for those atoms refined anisotropically are calculated by using the formula given by: Hamilton, W. C. *Acta Crystallogr.* **1959**, *12*, 609.
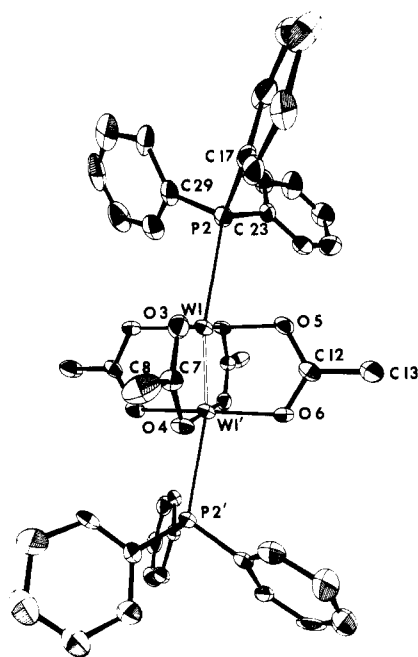

Figure 1. ORTEP drawing of $W_2(O_2C$-t-$Bu)_4 \cdot 2PPh_3$. Each non-hydrogen atom is represented by a thermal-vibration ellipsoid enclosing 50% of its electron density.

distances and angles are listed in Table III.

In the monoclinic space group $C2/c$ with $Z = 4$, crystallographic inversion symmetry is imposed on **3**. An ORTEP drawing of the adduct is shown in Figure 1. For viewing purposes, we have

Table III. Selected Bond Distances (Å) and Angles (deg) in $W_2(O_2C$-t-$Bu)_4 \cdot 2PPh_3$

A	B	dist	A	B	dist
W(1)	W(1)	2.218 (1)	C(13)	C(16)	1.456 (19)
W(1)	P(2)	2.965 (3)	C(17)	C(18)	1.404 (15)
W(1)	O(3)	2.080 (7)	C(17)	C(22)	1.400 (15)
W(1)	O(4)	2.093 (7)	C(18)	C(19)	1.378 (17)
W(1)	O(5)	2.098 (7)	C(19)	C(20)	1.363 (18)
W(1)	O(6)	2.079 (7)	C(20)	C(21)	1.385 (18)
P(2)	C(17)	1.823 (12)	C(21)	C(22)	1.395 (16)
P(2)	C(23)	1.833 (11)	C(23)	C(24)	1.372 (16)
P(2)	C(29)	1.836 (11)	C(23)	C(28)	1.391 (16)
O(3)	C(7)	1.295 (12)	C(24)	C(25)	1.398 (18)
O(4)	C(7)	1.292 (12)	C(25)	C(26)	1.396 (18)
O(5)	C(12)	1.298 (12)	C(26)	C(27)	1.358 (19)
O(6)	C(12)	1.290 (12)	C(27)	C(28)	1.376 (18)
C(7)	C(8)	1.492 (15)	C(29)	C(30)	1.376 (17)
C(8)	C(9)	1.539 (16)	C(29)	C(34)	1.409 (17)
C(8)	C(10)	1.525 (18)	C(30)	C(31)	1.376 (17)
C(8)	C(11)	1.502 (18)	C(31)	C(32)	1.389 (22)
C(12)	C(13)	1.480 (16)	C(32)	C(33)	1.369 (21)
C(13)	C(14)	1.549 (22)	C(33)	C(34)	1.424 (18)
C(13)	C(15)	1.468 (22)			

A	B	C	angle	A	B	C	angle
W(1)	W(1)	P(2)	164.4 (1)	C(12)	C(13)	C(14)	104.4 (11)
W(1)	W(1)	O(4)	89.2 (2)	C(12)	C(13)	C(15)	112.5 (11)
W(1)	W(1)	O(6)	91.2 (2)	C(12)	C(13)	C(16)	113.7 (11)
P(2)	W(1)	O(4)	77.8 (2)	C(14)	C(13)	C(15)	102.0 (16)
P(2)	W(1)	O(6)	96.9 (2)	C(14)	C(13)	C(16)	103.9 (13)
W(1)	P(2)	C(17)	116.2 (4)	C(15)	C(13)	C(16)	118.2 (16)
W(1)	P(2)	C(23)	115.6 (4)	P(2)	C(17)	C(18)	124.8 (9)
W(1)	P(2)	C(29)	110.5 (4)	P(2)	C(17)	C(22)	116.8 (8)
C(17)	P(2)	C(23)	103.5 (5)	C(18)	C(17)	C(22)	118.2 (11)
C(17)	P(2)	C(29)	108.3 (5)	C(17)	C(18)	C(19)	121.0 (11)
C(23)	P(2)	C(29)	101.4 (5)	C(18)	C(19)	C(20)	120.5 (11)
W(1)	O(3)	C(7)	119.1 (6)	C(19)	C(20)	C(21)	120.0 (12)
W(1)	O(5)	C(12)	119.2 (6)	C(20)	C(21)	C(22)	120.6 (12)
O(3)	C(7)	O(4)	119.7 (9)	C(17)	C(22)	C(21)	119.6 (11)
O(3)	C(7)	C(8)	120.0 (9)	P(2)	C(23)	C(24)	116.6 (8)
O(4)	C(7)	C(8)	120.3 (9)	P(2)	C(23)	C(28)	124.3 (9)
C(7)	C(8)	C(9)	109.6 (9)	C(24)	C(23)	C(28)	119.0 (11)
C(7)	C(8)	C(10)	106.9 (10)	C(23)	C(24)	C(25)	121.8 (11)
C(7)	C(8)	C(11)	109.7 (11)	C(24)	C(25)	C(26)	118.0 (12)
C(9)	C(8)	C(10)	109.9 (11)	C(25)	C(26)	C(27)	119.7 (12)
C(9)	C(8)	C(11)	110.1 (10)	C(26)	C(27)	C(28)	122.2 (12)
C(10)	C(8)	C(11)	110.5 (11)	C(23)	C(28)	C(27)	119.2 (12)
O(5)	C(12)	O(6)	120.8 (9)	C(23)	C(29)	C(30)	115.7 (9)
O(5)	C(12)	C(13)	118.7 (9)	P(2)	C(29)	C(34)	124.2 (10)
O(6)	C(12)	C(13)	120.4 (9)	C(30)	C(29)	C(34)	120.0 (11)

deleted the *tert*-butyl methyl groups from the figure. The W_2-$(O_2C$-t-$Bu)_4$ portion of the adduct has virtual D_{4h} symmetry, and the W–W bond length is 2.218 (1) Å. This distance falls within the range of known tungsten–tungsten quadruple bond lengths,[15] i.e., 2.155 (2)–2.375 (1) Å. It is 0.13 Å longer than the Mo–Mo bond length (2.088 (1) Å) found in $Mo_2(O_2C$-t-$Bu)_4$[13] and comparable to the W–W bond lengths (2.240 (1) and 2.243 (1) Å) found in $W_2(O_2CCF_3)_4 \cdot 2PPh_3$.[11] The tungsten–phosphorus distance in **3** is 2.965 (3) Å, and the W–W–P angle is 164.4 (1)°. The W–P bond is clearly a weak one, and we find (vide infra) that the phosphine ligands are extensively dissociated in solution. The remaining bond distances and angles appear normal and do not merit further discussion.

Physicochemical Properties. Dimers **1** and **2** are extremely air-sensitive bright yellow solids. They are considerably more air sensitive than their molybdenum analogues, decomposing exothermically to black powders within seconds after exposure to laboratory air. Adduct **3** is slightly more robust; it lasts several minutes in air. **1** is *very* soluble in ethereal solvents, moderately soluble in toluene and acetonitrile, and slightly soluble in hexane. **2** is slightly soluble in THF and acetonitrile, but solutions in the latter solvent are unstable; the characteristic yellow color of **2**

(15) Cotton, F. A.; Felthouse, T. R. *Inorg. Chem.* **1981**, *20*, 3880 and references therein.

changes to brown after several hours. Neither **1** nor **2** can be sublimed (10^{-4} torr, 100–150 °C) without appreciable losses.

A strong parent ion multiplet, characteristic of the W_2 unit, was observed in the electron-impact (70-eV) mass spectrum of each complex. It is important to note that samples of **2**, prepared as described above, did *not* show any multiplet patterns corresponding to partially exchanged species, i.e., $W_2(O_2CCF_3)_{4-x}$-$(O_2CMe)_x$. The fragmentation patterns of both alkanecarboxylates are complex. In the acetate,[16] for example, we see loss of $CH_3CO_2\cdot$, $CH_3CO\cdot$, and $CH_2=C=O$ from the parent. Major ions, with tungsten atom weights totaling 368, are observed at m/e 520, 478, 459, and 432, which correspond to W_2-$(O_2CMe)_2(OH)_2^+$, $W_2(O_2CMe)(OH)_3^+$, $W_2(O_2CMe)O_2^+$, and $W_2O_4^+$, respectively.

The vibrational spectra of **1**, **2**, and **3** have been examined by IR and Raman spectroscopy. The infrared spectrum of each dimer is in accord with bidentate carboxylate coordination. Strong asymmetric CO_2 vibrations are observed at 1472, 1485, and 1485 cm^{-1}, for **1**, **2**, and **3**, respectively.

The most interesting feature of the vibrational spectra of quadruply metal–metal bonded complexes is that vibration which corresponds mainly to M$\overset{4}{-}$M stretching, ν(M–M). This totally symmetric vibration is Raman active and was observed in the Raman spectra of **1**, **2**, and **3**. The W–W stretching mode in the pivalate dimer (**1**) appears at 313 (3) cm^{-1} and shifts to 287 (3) cm^{-1} in the triphenylphosphine adduct (**3**). The magnitude and direction of the shift in ν(M–M) were anticipated from our earlier work with $W_2(O_2CCF_3)_4$ and $W_2(O_2CCF_3)_4\cdot2PPh_3$[11] and the data collected by Cotton and Norman on $Mo_2(O_2CCF_3)_4$ and Mo_2-$(O_2CCF_3)_4\cdot2py$.[17,18] A decrease in ν(M–M) is associated with an increase in the M–M distance. Using arguments similar to those presented earlier,[11] we estimate that the M–M bond length in **1** is in the range of 2.19–2.20 Å.[19] In the acetate dimer (**2**) ν(M–M) is located at 304 (3) cm^{-1}. The proton NMR spectra of $W_2(O_2C$-t-$Bu)_4$ and $W_2(O_2C$-t-$Bu)_4\cdot2PPh_3$ show single, sharp t-Bu resonances at δ 1.40 and 1.41, respectively. The $^{31}P\{^1H\}$ NMR spectrum of the adduct shows a single resonance 7.2 ppm downfield from the resonance position of the free ligand in the same solvent (benzene-d_6). No tungsten-183 satellites ($I = {}^1/_2$; 14.4% abundant) were observed in the phosphorus spectrum. The latter observations suggest weak coordination of PPh$_3$ in solution, consistent with the long W–P bond (2.965 (3) Å) observed in the solid state. The proton NMR spectrum of $W_2(O_2CMe)_4$ was measured in tetrahydrofuran-d_8. A single sharp methyl resonance was observed at δ 2.91. Again, no mixed-ligand species were detected.

The ^{183}W NMR spectrum of **1** (ca. 1 M in THF) consists of a single, sharp (fwhm $\cong$ 1 Hz) resonance at δ +5954 vs. 2 M Na_2WO_4 in D_2O (δ 0.0).[20] This is 800 ppm *upfield* from the ^{183}W NMR resonance of $W_2(O_2CCF_3)_4$ (δ +6760) in the same solvent at the same concentration.[11] The data suggest that there is an increase in electron density at the tungsten centers when CF$_3$ (electron withdrawing) is replaced by t-Bu (electron releasing) on the carboxylate framework. Inductive effects due to the carboxylate ligands are also evident in the UV photoelectron spectra of these complexes. In **1**, the δ and π ionizations are observed at 5.93 and 7.65 eV,[21] respectively, while the corresponding ionizations in $W_2(O_2CCF_3)_4$ are located at 7.83 and 9.43 eV.[22]
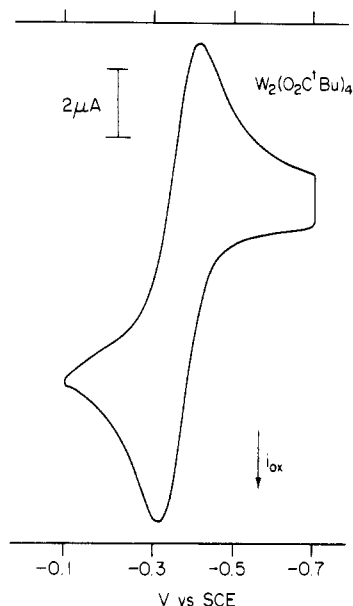
(16) The fragmentation of **2** is similar to that of $Mo_2(O_2Me)_4$. See: Hochberg, E.; Walks, P.; Abbot, E. H. *Inorg. Chem.* **1974**, *13*, 1824.
(17) Cotton, F. A.; Norman, J. G., Jr. *J Coord. Chem.* **1971**, *1*, 161.
(18) Cotton, F. A.; Norman, J. G., Jr. *J. Am. Chem. Soc.* **1972**, *94*, 5697.
(19) The W–W bond length in $[W_2(O_2CEt)_4]_n$ is 2.189 (1) Å. See: Chisholm, M. H.; Chiu, H. T.; Huffman, J. C. *Polyhedron*, **1984**, *3*, 759.
(20) Gansow, O. A.; Ho, R. K. C.; Klemperer, W. G. *J. Organomet. Chem.* **1980**, *187*, C27. Chemical shifts to the high-frequency side of the reference are assigned positive values.
(21) Lichtenberger, D. L.; Blevins, C. H.; Sattelberger, A. P.; McCarley, R. E., in preparation.
(22) Lichtenberger, D. L.; Blevins, C. H.; Sattelberger, A. P.; Santure, D. J., in preparation.

Figure 2. Cyclic voltammogram of ca. 2 mM $W_2(O_2C$-t-$Bu)_4$ in 0.1 M tetrabutylammonium tetrafluoroborate–acetonitrile solution (platinum-disk electrode; sweep rate 250 mV s^{-1}).

Table IV. $E_{1/2}$ Values for $Mo_2(O_2CR)_4$ and $W_2(O_2CR)_4$ Complexes in Acetonitrile (V vs. SCE)

complex	$E_{1/2}$	complex	$E_{1/2}$
$Mo_2(O_2C$-n-$Pr)_4$	+0.39[a]	$W_2(O_2C$-t-$Bu)_4$	−0.37[b]
$Mo_2(O_2C$-t-$Bu)_4$	+0.38[b]	$W_2(O_2CMe)_4$	−0.40[b]

[a] Reference 28; 0.1 M [Bu_4N]ClO_4 as supporting electrolyte, platinum working electrode. [b] This work; 0.1 M [Bu_4N]BF_4 as supporting electrolyte, platinum working electrode.

Electrochemistry of $W_2(O_2C$-t-$Bu)_4$ and $W_2(O_2CMe)_4$.[23] Cyclic voltammetry at 25 ± 2 °C on **1** and **2** was performed by employing a polished platinum-disk electrode in purified, O_2-free acetonitrile, which was 0.1 M in tetrabutylammonium tetrafluoroborate. Sample concentrations were varied from 2.0 to 10.0 mM. The potential range investigated was from −2.0 to +1.0 V vs. the Ag/Ag^+ (0.1 M $AgNO_3$ in CH_3CN) couple. At approximately −0.1 V in cyclic sweeps initiated at −1.0 V, an oxidation wave was observed for both of the tungsten samples. At potential sweep rates between 100 and 600 mV s^{-1}, the ratio of anodic and cathodic peak currents, i_{pa}/i_{pc}, was unity. A representative cyclic voltammogram of **1** is shown in Figure 2. The potential separation, ΔE_p, between anodic and cathodic peaks was in all cases greater than 60 mV and varied with sweep rate; at 250 mV s^{-1}, ΔE_p was in the range 80–100 mV. These electrochemical properties can be viewed as being in accord with quasi-reversible electron-transfer processes.[24,25] However, we (and others)[26] find that the known reversible couple ferrocene/ferrocenium exhibits electrochemical behavior similar to that described above under the same experimental conditions. We conclude that the electron-transfer processes in $W_2(O_2CR)_4$ complexes approach electrochemical reversiblility.

In Table IV we have collected the $E_{1/2}$ values of **1**, **2**, Mo_2-$(O_2C$-t-$Bu)_4$, and $Mo_2(O_2C$-n-$Pr)_4$. The $E_{1/2}$ values are the average of $E_{pa} + E_{pc}$, and we have converted our $E_{1/2}$ values for **1**, **2**, and $Mo_2(O_2C$-t-$Bu)_4$, which were measured vs. Ag/Ag^+, to the SCE scale.[27] The $E_{1/2}$ value for $Mo_2(O_2C$-n-$Pr)_4$ was taken from

(23) Reliable electrochemical data could not be obtained on $W_2(O_2CCF_3)_4$ because of its instability in the electrolyte solution.
(24) Murray, R. W.; Reilley, C. N. "Electroanalytical Principles"; Interscience: New York, 1963.
(25) Nicholson, R. S. *Anal. Chem.* **1965**, *37*, 1351.
(26) Brisdon, B. J.; Conner, K. A.; Walton, R. A. *Organometallics* **1983**, *2*, 1159.
(27) A correction factor of 0.294 V, the difference in $E_{1/2}$ values for ferrocene vs. the two reference electrodes, was used.
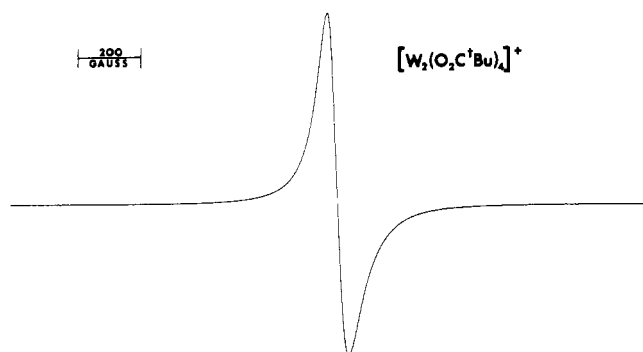
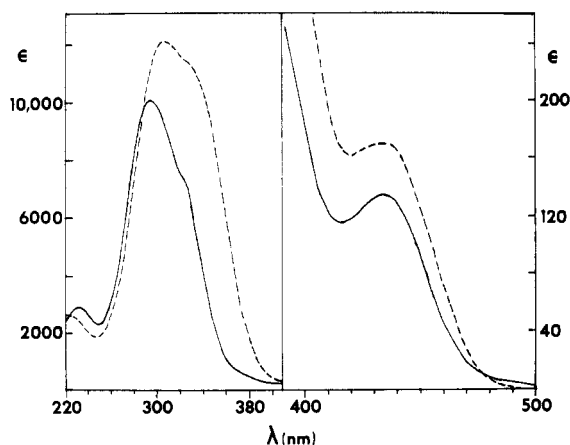**Figure 3.** X-Band ESR spectrum of polycrystalline [W₂(O₂C-*t*-Bu)₄]I at 25 °C.

Figure 4. Electronic absorption spectra of Mo₂(O₂CCF₃)₄ (‐‐) and Mo₂(O₂C-*t*-Bu)₄ (—) in THF. Extinction coefficients (ϵ) are in M⁻¹ cm⁻¹.

Figure 5. Electronic absorption spectra of W₂(O₂CCF₃)₄ (‐‐) and W₂(O₂C-*t*-Bu)₄ (—) in THF.

Table V. Electronic Absorption Spectra of M₂(O₂CR)₄ Compounds[a,b]

species	abs max, nm	ν, cm⁻¹	ϵ, M⁻¹ cm⁻¹
W₂(O₂CCF₃)₄	395	25 300	14 500
	~426 sh	23 500	
	~688	14 500	~1.7
W₂(O₂C-*t*-Bu)₄	377	26 500	12 600
	735	13 600	~1.0
Mo₂(O₂CCF₃)₄	306	32 700	12 100
	~333 sh	30 000	
	435	23 000	170
Mo₂(O₂C-*t*-Bu)₄	295	33 900	10 000
	~326 sh	30 700	
	434	23 000	136
MoW(O₂C-*t*-Bu)₄	334	29 900	13 000
	440	22 700	290

[a] All spectra were recorded in THF. [b] sh ≡ shoulder.

the work of Cotton and Pedersen.[28]

One fact is clearly evident from the data in Table IV: ditungsten tetracarboxylates are much easier to oxidize than their molybdenum counterparts. The difference in $E_{1/2}$ values (ca. 0.75 V) as well as the negative potentials associated with oxidation of the tungsten dimers is probably sufficient to explain why W₂(O₂CR)₄ complexes cannot be isolated by variants of reaction 4.

$$2Mo(CO)_6 + 4HO_2CR \xrightarrow{\Delta} Mo_2(O_2CR)_4 + 12CO + 2H_2 \tag{4}$$
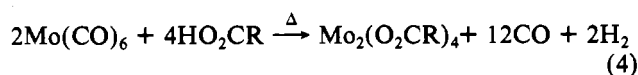
It is possible to oxidize **1** chemically with elemental iodine in benzene to give a gray, microcrystalline, paramagnetic solid (reaction 5). The infrared spectrum (Fluorolube mull) of

$$\underset{\textbf{1}}{W_2(O_2C\text{-}t\text{-}Bu)_4} + 0.5I_2 \xrightarrow{PhH} \underset{\textbf{4}}{[W_2(O_2C\text{-}t\text{-}Bu)_4]I} \tag{5}$$
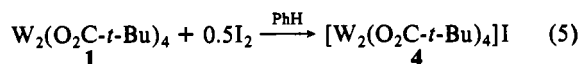
[W₂(O₂C-*t*-Bu)₄]I (**4**) is nearly superimposable with that of the parent, indicating that **4** is formed with retention of the carboxylate framework. The solid-state ESR spectrum of polycrystalline **4** at 25 °C is shown in Figure 3; a single narrow, virtually isotropic signal with $g = 1.794$ is observed. Hyperfine coupling to tungsten-183 was not resolved. The g value obtained for **4** may be compared to those obtained for [Mo₂(O₂C-*t*-Bu)₄]I₃ ($g = 1.93$) and [MoW(O₂C-*t*-Bu)₄]I ($g = 1.877$).[29] The decrease in g as the number of tungsten atoms increases from 0 to 2 was predicted several years ago by Cotton and Pedersen,[30] and the reader is referred to their paper for a qualitative discussion of the relationship between g factors and electronic structure in multiply
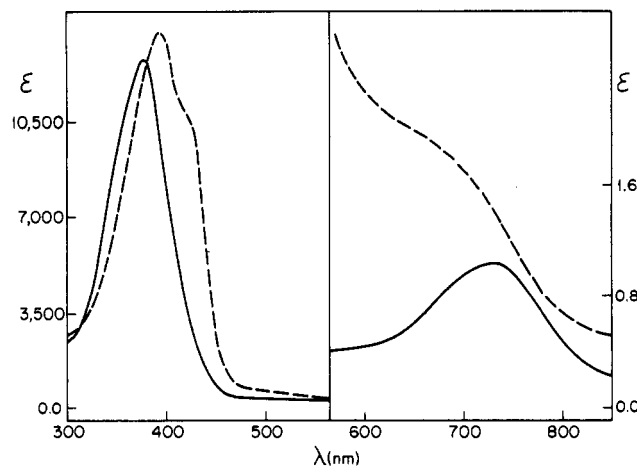
metal–metal-bonded complexes.

Electronic Absorption Spectra of M₂(O₂CR)₄ Complexes. The most interesting, and most studied, feature of the electronic absorption spectra of quadruply metal–metal-bonded complexes is the $\delta \rightarrow \delta^*$, $^1A_{1g} \rightarrow {}^1A_{2u}$ transition.[31-33] The electronic absorption spectra of Mo₂(O₂CCF₃)₄ and Mo₂(O₂C-*t*-Bu)₄, both recorded in THF, are shown in Figure 4. The weak bands at ca. 434 nm (~23 000 cm⁻¹) in both spectra have been assigned as the $\delta \rightarrow \delta^*$ transitions. A detailed discussion of the data that led to this assignment can be found in the paper by Martin et al.[14]

Figure 5 shows the electronic absorption spectra (in THF) of W₂(O₂CCF₃)₄ and W₂(O₂C-*t*-Bu)₄. No other electronic transitions were detected out to 2500 nm (4000 cm⁻¹). Band maxima and extinction coefficients for all M₂(O₂CR)₄ molecules are listed in Table V. Our first inclination, after comparing these spectra with those of their molybdenum homologues (Figure 4), was to assign the weak bands at ca. 688 nm (14 535 cm⁻¹) in the W₂(O₂CCF₃)₄ spectrum and at 735 nm (13 605 cm⁻¹) in the W₂(O₂C-*t*-Bu)₄ spectrum as the $\delta \rightarrow \delta^*$, $^1A_{1g} \rightarrow {}^1A_{2u}$ transitions. In due course, these assignments were rejected for the following reasons: (1) The intensities of the 688- and 735-nm bands ($\epsilon \approx 1.0$ M⁻¹ cm⁻¹, $f \approx 10^{-5}$) are simply too low for fully allowed transitions. They are 2 orders of magnitude weaker than the intensities of the $\delta \rightarrow \delta^*$ transitions in the Mo₂(O₂CR)₄ spectra ($\epsilon \approx 150$ M⁻¹ cm⁻¹, $f \approx 10^{-3}$). (2) In the M₂Cl₈⁴⁻,[34,35] M₂(CH₃)₈⁴⁻,[34] M₂Cl₄(PMe₃)₄,[34] and M₂(mhp)₄[34] (mhp = anion of 2-hydroxy-6-methylpyridine)

(28) Cotton, F. A.; Pedersen, E. *Inorg. Chem.* **1975**, *14*, 399.
(29) McCarley, R. E.; Templeton, J. L.; Colburn, T. J.; Katovic, V.; Hoxmeier, R. J. In "Inorganic Compounds with Unusual Properties"; King, R. B., Ed.; American Chemical Society: Washington, DC, 1976; Adv. Chem. Ser. No. 150, pp 318–334.
(30) Cotton, F. A.; Pedersen, E. *J. Am. Chem. Soc.* **1975**, *97*, 303.

(31) Trogler, W. C.; Gray, H. B. *Acc. Chem. Res.* **1978**, *11*, 232.
(32) Reference 4, pp 390–413.
(33) Wambaugh, J. "The Delta Star"; Morrow: New York, 1983.
(34) Manning, M. C.; Trogler, W. C. *J. Am. Chem. Soc.* **1983**, *105*, 5311 and references therein.
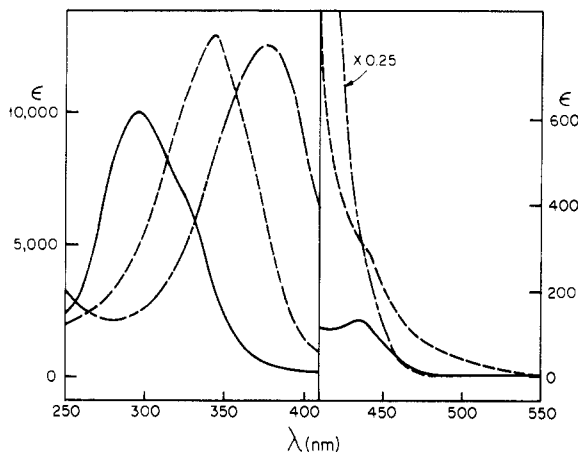(35) Schrock, R. R.; Sturgeoff, L. G.; Sharp, P. R. *Inorg. Chem.* **1983**, *22*, 2801.

Figure 6. Electronic absorption spectra of Mo$_2$(O$_2$C-t-Bu)$_4$ (—), MoW-(O$_2$C-t-Bu)$_4$ (-- --), and W$_2$(O$_2$C-t-Bu)$_4$ (— —).

systems (M = Mo, W), the difference in $\delta \rightarrow \delta^*$ transition energies between homologues is 2490, 2700, 1980, and 2300 cm^{-1}, respectively. The $\delta \rightarrow \delta^*$ transition for M = W lies at lower energy in each of these cases, and it is more intense (usually by 20–25%). If the weak bands in the W$_2$(O$_2$CR)$_4$ spectra were the $\delta \rightarrow \delta^*$ transitions, the difference in $\delta \rightarrow \delta^*$ transition energies for M$_2$-(O$_2$CR)$_4$ homologues would be ca. 9000 cm^{-1}, which seems much too large. (3) When we compare the spectra of Mo$_2$Cl$_8$$^{4-}$ and Mo$_2$(O$_2$C-t-Bu)$_4$,[34] we note that the $\delta \rightarrow \delta^*$ transition blue shifts from 19 300 cm^{-1} in the octachloride to 23 040 cm^{-1} in the pivalate. The $\delta \rightarrow \delta^*$ transition in W$_2$Cl$_8$$^{4-}$ occurs[35] at 16 800 cm^{-1}. We find it difficult to believe that the $\delta \rightarrow \delta^*$ transition would shift to lower energy going from W$_2$Cl$_8$$^{4-}$ to W$_2$(O$_2$C-t-Bu)$_4$. (4) SCF–Xα–SW calculations performed in this laboratory on the model compounds Mo$_2$(O$_2$CH)$_4$ and W$_2$(O$_2$CH)$_4$ suggest that the $\delta \rightarrow \delta^*$ transitions of W$_2$(O$_2$CR)$_4$ compounds may actually occur at slightly higher energies than those of their molybdenum homologues.[36]

The evidence against assigning the weak bands in the 650–750-nm regions of the W$_2$(O$_2$CR)$_4$ spectra as the $\delta \rightarrow \delta^*$, $^1A_{1g} \rightarrow {}^1A_{2u}$ transitions is compelling and immediately raises two questions: (1) Where are the spin-allowed $\delta \rightarrow \delta^*$ transitions? (2) What electronic transition is responsible for the weak bands? We will answer both of these questions in due course, but first it is necessary to consider the high-energy regions of the M$_2$-(O$_2$CR)$_4$ spectra.

The proposed assignment for the most intense feature in the molybdenum spectra is $\delta \rightarrow \pi^*$ (OCO), $^1A_{1g} \rightarrow {}^1E_u$, i.e., a dipole-allowed, metal-to-lignd charge-transfer excitation.[37] This assignment is consistent with the R group dependence of the transition energy (see Table V), the high oscillator strength ($f \approx 0.2$) of the solution absorption band, and the SCF–Xα–DV calculations[38] on Mo$_2$(O$_2$CH)$_4$. The tungsten(II) carboxylate spectra are also in accord with this assignment. Going from Mo$_2$(O$_2$CR)$_4$ to W$_2$(O$_2$CR)$_4$, the $\delta \rightarrow \pi^*$ (OCO) transition red shifts by 7400 cm^{-1} (0.92 eV) when R = CF$_3$ or t-Bu. A shift of this magnitude is expected because the δ level rises by 0.7–1.0 eV going from Mo$_2$(O$_2$CR)$_4$ to W$_2$(O$_2$CR)$_4$[21,22] while the π^* level of the carboxylate remains at essentially the same energy.

In Figure 6 we show the solution (THF) absorption spectra of Mo$_2$(O$_2$C-t-Bu)$_4$, MoW(O$_2$C-t-Bu)$_4$,[29,39] and W$_2$(O$_2$C-t-Bu)$_4$. The δ ionization energies of these compounds, as measured by gas-phase UV photoelectron spectroscopy,[21] are 6.75, 6.34, and 5.93 eV, respectively; i.e., there is a uniform shift of 0.41 eV to lower binding energy as molybdenum is sequentially replaced by tungsten in the

M$_2$(O$_2$C-t-Bu)$_4$ framework. From Table V we see that the $\delta \rightarrow \pi^*$ (OCO) transition energy decreases by 0.49 eV going from Mo$_2$(O$_2$C-t-Bu)$_4$ to MoW(O$_2$C-t-Bu)$_4$ and by 0.42 eV going from MoW(O$_2$C-t-Bu)$_4$ to W$_2$(O$_2$C-t-Bu)$_4$. The agreement between the two experiments is quite satisfactory and provides further support for the $\delta \rightarrow \pi^*$ (OCO) assignments. The spectra of W$_2$(O$_2$CCF$_3$)$_4$, Mo$_2$(O$_2$CCF$_3$)$_4$, and Mo$_2$(O$_2$C-t-Bu)$_4$ also show a pronounced shoulder on the low-energy side of the $\delta \rightarrow \pi^*$ (OCO) absorption band. The origin of this transition is not known at the present time, and an assignment will require further experimental and theoretical study.

Let us return now to the first question posed above concerning the location of the spin-allowed $\delta \rightarrow \delta^*$ transition in the tungsten(II) carboxylate spectra. We think Figure 6 provides a satisfactory answer. In the Mo$_2$(O$_2$C-t-Bu)$_4$ spectrum, the $\delta \rightarrow \delta^*$ transition is a distinct band, well separated from the $\delta \rightarrow \pi^*$ (OCO) absorption band. In the MoW(O$_2$C-t-Bu)$_4$ spectrum, the $\delta \rightarrow \delta^*$ transition ($^1A_1 \rightarrow {}^1A_1$) is also visible at 440 nm but now it is only a weak shoulder on the low-energy side of the $\delta \rightarrow \pi^*$ (OCO) band. On the basis of these two observations it seems reasonable to propose that the $\delta \rightarrow \delta^*$ transition in the W$_2$-(O$_2$C-t-Bu)$_4$ spectrum is completely masked by the intense $\delta \rightarrow \pi^*$ (OCO) transition, which has red shifted 3400 cm^{-1} from its position in the MoW(O$_2$C-t-Bu)$_4$ spectrum.

The final question we need to address is an assignment for the weak bands in the W$_2$(O$_2$CR)$_4$ spectra (Figure 5). The extinction coefficients of these bands are in the range expected for singlet–triplet transitions, and the latter are expected to be more prominent in a ditungsten system because of the increase in spin–orbit coupling as we move down the periodic table. We are therefore inclined to assign the bands at 688 nm in the W$_2$(O$_2$-CCF$_3$)$_4$ spectrum and at 735 nm in the W$_2$(O$_2$C-t-Bu)$_4$ spectrum as the spin-forbidden $\delta \rightarrow \delta^*$, $^1A_{1g} \rightarrow {}^3A_{2u}$ transitions.[40] In principle this assignment can be tested by using single-crystal polarized spectroscopy because the $\delta \rightarrow \delta^*$, $^1A_{1g} \rightarrow {}^1A_{2u}$ transition is z polarized while the $\delta \rightarrow \delta^*$, $^1A_{1g} \rightarrow {}^3A_{2u}$ transition is x,y polarized. Such a test is welcome, but it will be very difficult because of the extreme air sensitivity of the W$_2$(O$_2$CR)$_4$ complexes.

Discussion

We have shown here that W$_2$(O$_2$C-t-Bu)$_4$ and W$_2$(O$_2$CMe)$_4$ can be prepared easily and in very good yields. The synthesis of **1** is modeled after that of W$_2$(O$_2$CCF$_3$)$_4$, and the only significant difference is in the workup of the product; i.e., the trifluoroacetate dimer can be sublimed directly from the crude reaction mixture while **1** is best isolated and purified by solution techniques. In either case, the yield of W$_2$(O$_2$CR)$_4$, based on WCl$_4$, is greater than 50%. Two other groups have independently developed small-scale syntheses of **1** using procedures similar to the one reported here.[35,41]

The synthesis of tungsten(II) acetate was more onerous. Several attempts to prepare **2** via reaction 6 were unsuccessful; mass

$$\text{WCl}_4 + 2\text{Na/Hg} + 2\text{NaO}_2\text{CMe} \xrightarrow{\text{THF}} \nrightarrow \text{W}_2(\text{O}_2\text{CMe})_4 \quad (6)$$

spectra of the black products obtained from these reactions did not show any **2**$^+$. We thought that these failures were due to the low solubility of sodium acetate in THF, and so, in our next experiments, we used a THF-soluble salt, viz., tetrabutylammonium acetate. From these, we obtained yellow-brown powders, but once again, mass spectral analysis failed to show **2**$^+$ and this synthetic approach was abandoned.

The successful synthesis of **2** was based on the premises (1) that W$_2$(O$_2$CCF$_3$)$_4$, like Mo$_2$(O$_2$CCF$_3$)$_4$,[42] would readily exchange

(36) Sattelberger, A. P.; Scioly, A., in preparation.
(37) Norman, J. G., Jr.; Kolari, H. J.; Gray, H. B.; Trogler, W. C. *Inorg. Chem.* **1977**, *16*, 987.
(38) Manning, M. C.; Holland, G. F.; Ellis, D. E.; Trogler, W. C. *J. Phys. Chem.* **1983**, *87*, 3083.
(39) Katovic, V.; Templeton, J. L.; Hoxmeier, R. J., McCarley, R. E. *J. Am. Chem. Soc.* **1975**, *97*, 5300.

(40) The $\delta \rightarrow \delta^*$, $^1A_{1g} \rightarrow {}^3A_{2u}$ and $^1A_{1g} \rightarrow {}^1A_{2u}$ transitions have been observed in the polarized crystal spectrum of Re$_2$(O$_2$C-t-Bu)$_4$Cl$_2$. Here the separation of the $^3A_{2u}$ and $^1A_{2u}$ states is ca. 4000 cm^{-1}. See: Martin, D. S.; Huang, H.-W.; Newman, R. A. *Inorg. Chem.* **1984**, *23*, 699.
(41) Girolami, G. S.; Mainz, V. V.; Andersen, R. A., submitted for publication.
(42) Teremoto, L.; Sasaki, Y.; Migita, K.; Iwaizumi, M.; Saito, K. *Bull. Chem. Soc. Jpn.* **1979**, *52*, 446.

with free carboxylate in solution and (2) that $W_2(O_2CMe)_4$, like $Mo_2(O_2CMe)_4$,[3] would be insoluble, or nearly so, in common organic solvents. The respective homologous pairs do indeed have similar properties, and the addition of tetrabutylammonium acetate to concentrated toluene solutions of $W_2(O_2CCF_3)_4$ results in the rapid precipitation of **2**. The latter *must* be isolated as quickly as possible because it decomposes if left in contact with the mother liquor. Liberal washing of the product with methylene chloride removes any mixed-ligand dimers and/or residual $[Bu_4N]O_2CR$ and provides a bright yellow powder that is pure by ^1H NMR and mass spectroscopy. It is worth noting that a similar approach for the synthesis of $W_2(O_2CH)_4$ was unsuccessful.

The electrochemical results (Table IV), optical spectra (Table V), and UV photoelectron spectra[10,21,22] all indicate a substantial destabilization of the δ component of the metal–metal bond in the tungsten dimers. The $W_2(O_2CR)_4$ compounds are much more susceptible to oxidation than their molybdenum analogues, and it is not very surprising that the syntheses that have evolved for ditungsten carboxylates are necessarily ones that do not involve potential oxidizing agents. It is very unlikely that $W_2(O_2CR)_4$ compounds were ever isolated from reactions involving carboxylic acids.[43] They may be intermediates in such reactions, but this has not yet been demonstrated.

With reliable syntheses for **1**, **2**, $W_2(O_2CCF_3)_4$, and a series of arenecarboxylate complexes,[44] including $W_2(O_2CPh)_4$,[12] now in hand, the synthetic part of the ditungsten tetracarboxylate story is almost complete. One of the remaining challenges is the preparation of tungsten(II) formate, $W_2(O_2CH)_4$. There is clearly no good reason to believe that this dimer should not exist, and efforts to prepare it are continuing.

Further work on the electronic structures of $W_2(O_2CR)_4$ complexes is in progress and will be reported in future publications.

Experimental Section

Reagents. Tungsten hexachloride (99.9%; Great Western Inorganics), molybdenum and tungsten hexacarbonyls (Pressure Chemical), triphenylphosphine (Orgmet), and trimethylacetic acid (99+%; Aldrich) were used without further purification. Tetrabutylammonium acetate was purchased from Tridom/Fluka and dried by azeotropic distillation with benzene. Tetrabutylammonium tetrafluoroborate (Fisher) was dried under dynamic vacuum (10^{-5} torr) at 50 °C for 24 h. Solvents were dried and purified by standard techniques under argon. Polymeric tungsten tetrachloride, $([WCl_4]_x)$,[35] $W_2(O_2CCF_3)_4$,[11] $MoW(O_2C-t-Bu)_4$,[29,39] $Mo_2(O_2CCF_3)_4$,[17] $Mo_2(O_2C-t-Bu)_4$,[29] and $Mo_2(O_2CMe)_4$[14] were prepared by literature procedures. Sodium pivalate, $NaO_2C-t-Bu$, was synthesized from trimethylacetic acid and freshly prepared sodium methoxide in methanol. The crude solid was washed with ether, azeotropically dried with benzene, filtered, washed with ether, and dried under high vacuum (10^{-5} torr) for 12 h.

Physical and Analytical Measurements. Elemental analyses were performed by Galbraith Laboratories, Knoxville, TN, and Schwarzkopf Microanalytical Laboratory, Woodside, NY.

Infrared measurements were obtained from Fluorolube-mulled samples between KBr plates on a Perkin-Elmer Model 1330 infrared spectrometer. Raman spectra were obtained on a Spex Ramalog system, equipped with a Spectra Physics Model 125 helium/neon laser, which served as a 6328-Å excitation source. Solid samples were sealed in evacuated melting point capillaries. Peak positions are accurate to ±3 cm^{-1}.

NMR spectra were obtained on Bruker WM-360 and JEOL FX90Q spectrometers. ^1H, $^{31}P\{^1H\}$, and ^{183}W NMR spectra were recorded at 360.1, 36.20, and 3.73 MHz, respectively. Benzene-d_6 was used as a lock solvent unless otherwise noted. Phosphorus and tungsten chemical shifts (δ) are in ppm relative to external 85% H_3PO_4 and 2 M Na_2WO_4 in D_2O, both of which are assigned to a δ value of 0.0. Negative chemical shifts are assigned to resonances at lower frequency (higher field) than the reference. ESR spectra were recorded on a Bruker 200E-SRC spectrometer operating at 9.64 GHz. The g value reported for $[W_2(O_2C-t-Bu)_4]I$ is relative to DPPH ($g = 2.0036$).

Mass spectra were obtained on a Finnigan Model 6021 mass spectrometer by the method of direct insertion. Probe temperatures of 100–200 °C and ionizing voltages of 40–70 eV were employed. Tungsten

isotope patterns were calculated by using a local program written by Steve Werness of the Department of Chemistry, The University of Michigan.

Electrochemical measurements were performed with a Hi-Tek Model DT 201 potentiostat and a Hi-Tek Model PPR1 wave form generator. A standard three-electrode geometry, coupled with a three-compartment electrochemical cell, was used for cyclic voltammetry (CV) experiments. The three cell compartments were separated by medium-porosity sintered-glass disks, and the reference electrode (a silver wire immersed in a 0.1 M $AgNO_3$–acetonitrile solution) was further isolated by a Luggin capillary. The total volume of the working electrode (Pt disk) compartment was ca. 5 mL. Because of the extreme air sensitivity of the tungsten(II) carboxylates, all CV experiments were done within the confines of a Vacuum Atmospheres HE43-2 drybox (Argon atmosphere), which was modified for external connections to the potentiostat, wave form generator, and an X-Y recorder.[45] The supporting electrolyte for all runs was tetrabutylammonium tetrafluoroborate.

UV–visible spectra were recorded on Cary Model 219 and Model 14 spectrophotometers. Solutions of known concentration were prepared from freshly recrystallized samples inside the drybox and transferred to 0.1- or 1.0-cm quartz cuvettes topped with gastight, 9-mm Fischer-Porter Solv-Seals. Spectra were recorded immediately after removal of the samples from the drybox; extinction coefficients were reproducible to ±10%. All spectra were recorded at 25 °C.

General Procedures. All preparations and operations involving tungsten(II) carboxylates were carried out under dry and oxygen-free conditions by using Schlenk or drybox techniques. Our drybox is a Vacuum Atmospheres Model HE43-2 equipped with a high-capacity purification train (MO-40V) and a Dri-Cold freezer operating at -40 °C.

$W_2(O_2C-t-Bu)_4$. In the drybox, a 500-mL, three-neck round-bottom Morton flask equipped with a mechanical stirring shaft and bearing, a N_2 gas inlet, and a stopper was charged with 16 g (49 mmol) of powdered $[WCl_4]_x$, 15 g (121 mmol) of $NaO_2C-t-Bu$, ca. 350 mL of cold (0 °C) purified THF, and 35 mL of 0.5 wt % sodium amalgam (104 mmol of Na). The sealed flask was removed from the drybox, connected to a source of N_2, and placed in an ice bath. The stirrer shaft was connected to the motor, and the mixture was stirred *vigorously* for 20 min at 0 °C and a further 2 h at room temperature. The color of the mixture changed from gray-green to blue-green and finally to a deep yellow-brown. The stirrer was then replaced with a stopper and the flask removed to the drybox where the contents were filtered through a 1–2-in. layer of Celite on a 150-mL medium-porosity sintered-glass frit. The Celite was rinsed with 50 mL of fresh THF, and the combined filtrate was stripped to dryness. The crude product was a powdery yellow-brown solid at this point.[46] This solid was extracted (4 × 50 mL) with hot (ca. 70 °C) toluene, and the extracts were filtered through a 150-mL medium frit. The tan solid on the frit was discarded, and the yellow-brown filtrate was reduced to ca. 70 mL with mild heating under vacuum. The resultant suspension was placed in the freezer and cooled to -40 °C for 8 h. Crude yellow $W_2(O_2C-t-Bu)_4$ was collected on a glass frit and washed with hexane (2 × 30 mL). The powder was recrystallized from hot toluene (10 mL/g of solid) and the solution slowly cooled to room temperature and subsequently to -40 °C. The bright yellow needles obtained were filtered off, washed once with 20 mL of cold (-40 °C) toluene and twice with 30 mL of hexane, and dried in vacuo; yield ca. 13 g or 65% based on WCl_4.

Anal. Calcd for $W_2(O_2C-t-Bu)_4$ ($W_2O_8C_{20}H_{36}$): C, 31.11; H, 7.70; W, 47.62. Found: C, 31.92; H, 4.78; W, 47.54. ^1H NMR (C_6D_6, 360.1 MHz; ppm): 1.40 (s). ^{183}W NMR (THF, 3.73 MHz; ppm): +5954 (s). IR (Fluorolube mull; cm^{-1}): 1472 ($\nu_{asym}(CO_2)$). Raman (solid, 6328-Å excitation; cm^{-1}): 313 ($\nu_{sym}(W-W)$). MS (70 eV): m/e 772 (P$^+$), 757 (P – CH$_3^+$). UV-vis (THF; λ_{max}, nm): 337 (ϵ 1.26 × 10^4), 737 (ϵ 1.0).

$W_2(O_2C-t-Bu)_4\cdot2PPh_3$. $W_2(O_2C-t-Bu)_4$ (1.0 g, 1.3 mmol) was dissolved in 15 mL of hot toluene. Triphenylphosphine (0.679 g, 2.59 mmol, dissolved in a minimal amount of toluene, was added to the tungsten solution, which rapidly turned yellow-orange. As the solution cooled, a yellow-orange solid precipitated. The suspension was placed in the freezer (2 h, -40 °C) to complete the precipitation. The solid was collected by filtration, washed (3 × 2 mL) with hexane, and dried in vacuo; yield 1.35 g, 80%.

Anal. Calcd for $W_2(O_2C-t-Bu)_4\cdot2PPh_3$ ($W_2O_8P_2C_{56}H_{66}$): C, 51.86; H, 5.13; W, 28.35. Found: C, 51.59; H, 5.07; W, 28.19. ^1H NMR (C_6D_6, 360.1 MHz; ppm): 1.41 (s, $C(CH_3)_3$). $^{31}P\{^1H\}$ NMR (C_6D_6, 36.20 MHz; ppm): +0.2 (s). IR (Fluorolube mull; cm^{-1}): 1485

(43) (a) Cotton, F. A.; Jeremic, M. *Synth. Inorg. Met.-Org. Chem.* **1971**, *1*, 265. (b) Holste, G. *Z. Anorg. Allg. Chem.* **1973**, *398*, 249.
(44) Cotton, F. A.; Wang, W. *Inorg. Chem.* **1984**, *23*, 1604.

(45) These experiments were performed at Oakland University, Rochester, MI. The hospitality and assistance of Professor R. C. (Craig) Taylor are gratefully acknowledged.
(46) If the solid is tacky, 50 mL of hexane is added and the slurry is evaporated to dryness.

$(\nu_{asym}(CO_2))$. Raman (solid, 6328-Å excitation; cm⁻¹): 287 (ν_{sym}(W–W)).

[W₂(O₂C-*t*-Bu)₄]I. W₂(O₂C-*t*-Bu)₄ (1.0 g, 1.3 mmol) was dissolved in 40 mL of benzene. With constant stirring, 0.16 g (0.65 mmol) of I₂ dissolved in 5 mL of benzene was added dropwise to the tungsten solution. After 3 h, a light gray solid was isolated by filtration, washed several times with fresh benzene and then hexane, and dried in vacuo; yield 1.1 g, 95%.

Anal. Calcd for W₂O₈C₂₀H₃₆I: C, 26.72; H, 4.37; I, 14.11. Found: C, 26.92; H, 4.20; I, 14.85. IR (Fluorolube mull; cm⁻¹): 1491 (ν_{asym}(CO₂)). ESR (solid, 25 °C, 9.64 GHz): g_{iso} = 1.794.

W₂(O₂CMe)₄. (N.B. This procedure must be followed as closely as possible to obtain a pure product in the quoted yield.) Freshly sublimed W₂(O₂CCF₃)₄ (1.0 g, 1.22 mmol) was dissolved in 5 mL of 60 °C toluene with stirring. A suspension of 1.5 g (5 mmol) of powdered tetrabutyl-ammonium acetate in 10 mL of toluene was added, in one portion, to the tungsten solution. Precipitation of a bright yellow solid occurred within a few seconds after the addition. The mixture was stirred vigorously for a total of 30 s and then filtered rapidly through a 30-mL medium-porosity sintered-glass frit. The yellow solid was washed successively with 3 × 10 mL of methylene chloride and 2 × 10 mL of hexane and then dried in vacuo; yield 0.65–0.70 g, 80–90%.

Anal. Calcd for W₂O₈C₈H₁₂: C, 15.91; H, 2.00. Found: C, 16.41; H, 2.11. ¹H NMR (THF-*d₈*, 360.1 MHz; ppm): 2.91 (s). IR (Fluorolube mull; cm⁻¹): 1485 (ν_{asym}(CO₂)). Raman (solid, 6328-Å excitation; cm⁻¹): 304 (ν_{sym}(W–W)). UV–vis (THF, λ_{max}, nm): 375 (ϵ 1.50 × 10⁴). MS (70 eV): *m/e* 604 (P⁺) (see text).

X-ray Structure Determination of W₂(O₂C-*t*-Bu)₄·2PPh₃.⁴⁷ Large, well-formed yellow-orange blocks were obtained by slow cooling of a saturated toluene solution. Inside a nitrogen-filled glovebag, a small fragment of 0.1-mm maximum dimension was cleaved, mounted on a

glass fiber with silicon grease, and transferred to the liquid-nitrogen boil-off cooling system of the diffractometer. A systematic search of a limited hemisphere of reciprocal space revealed diffraction maxima that could be indexed as monoclinic, with systematic absences suggesting space group *C2/c* or *Cc*. Successful solution and refinement of the structure indicated the centrosymmetric choice was correct.

Diffraction data were collected at −163 ± 4 °C, and the structure was solved by a combination of Patterson, difference Fourier, and full-matrix least-squares refinement techniques. Several of the hydrogen atoms were located in a difference Fourier map phased on the refined non-hydrogen parameters, but attempts to refine them were unsuccessful. For this reason, all hydrogens were included as fixed atom contributors, by using idealized positions.

A final difference Fourier map contained several peaks of magnitude 1.8–2.4 e Å⁻³ in the vicinity of the tungsten and numerous peaks of magnitude 0.6–1.2 e Å⁻³ elsewhere.

(47) General procedures have been described in a previous publication. See: Huffman, J. C.; Lewis, L. N.; Caulton, K. G. *Inorg. Chem.* **1980**, *19*, 2755.

Contribution from the Department of Chemistry, The University of Michigan, Ann Arbor, Michigan 48109

Air Oxidation of the CpMo(CO)₃⁻ Anion. Molecular Structure of the (η²-Carbonato)dicarbonylcyclopentadienylmolybdenum(II) Anion, CpMo(CO)₂(η²-O₂CO)⁻

M. DAVID CURTIS* and KYOUNG R. HAN

Air (or dioxygen) reacts with the CpMo(CO)₃⁻ anion in acetone solution to give initially the deep red carbonato anion CpMo(CO)₂(η²-O₂CO)⁻. This anion may be isolated as the tetraethylammonium salt. Upon continued reaction with O₂, the carbonato anion is further oxidized to Mo₂O₇²⁻, which precipitates with the counterion in essentially quantitative yield. No other metal-containing species are detected in solution. The crystal structure of [Et₄N][CpMo(CO)₂(η²-O₂CO)] has been determined: triclinic, space group $P\bar{1}$ (No. 2); *a*, *b*, *c* (Å) = 8.103 (3), 11.824 (3), 9.572 (4); α, β, γ (deg) = 90.12 (3), 93.18 (3), 90.52 (3); *V* = 915.6 (6) Å³; *Z* = 2. The structure was solved by a Patterson and successive difference maps to *R* = 0.042, R_w = 0.051 based on 3091 data with *I* > 3σ(*I*). The anion has the typical four-legged piano stool structure. Some average bond distances (Å): M—CO, 1.94; Mo—O, 2.13; O—C, 1.31; O=C, 1.229 (5).

Introduction

Oxidation reactions, especially those involving metal-catalyzed reactions of dioxygen, are receiving renewed interest.[1,2] In order to understand the interaction of dioxygen with coordinated ligands in a catalytic cycle, some knowledge of such interactions in stoichiometric reactions is necessary. Molybdenum is widely associated with catalysis of redox reactions in both biological and industrial processes and displays a wide range of stable oxidation states.[3] It is therefore important to determine the ways in which

dioxygen interacts with ligands coordinated to molybdenum.

Cousins and Green[4] have investigated the reactions of dioxygen with a variety of cyclopentadienyl (Cp) compounds of molybdenum. Their results are summarized in Scheme I. It is interesting to note that Cp₂Mo₂(CO)₆ reacts to give (CpMoO₂)₂ and CpMoO₂Cl in the presence of chloroform. Cousins and Green also report that the hydride CpMo(CO)₃H reacts to give the dioxide dimer (CpMoO₂)₂, albeit in low yield. The major product

(1) (a) Voge, H. H.; Adama, C. R. *Adv. Catal.* **1967**, *17*, 151. (b) Grasselli, R. K.; Burrington, J. D. *Adv. Catal.* **1981**, *30*, 133.

(2) Sheldon, R. A.; Kochi, J. "Metal Catalyzed Oxidation of Organic Compounds"; Academic Press: New York, 1981.

(3) (a) Dolphin, D., Ed. "Biometric Chemistry"; American Chemical Society: Washington, DC, 1980; Adv. Chem. Ser. No. 191. (b) Massoth, F. E. *Adv. Catal.* **1978**, *27*, 266. (c) Barry, H. F., Mitchell, P. C. H., Eds. *Chem. Uses Molybdenum, Proc. Int. Conf., 4th* **1982**.

(4) Cousins, M.; Green, M. L. H. *J. Chem. Soc.* **1964**, 1567; *J. Chem. Soc. A* **1969**, 16.